



COVID-19–Associated Bone Marrow Necrosis—A Case Report

Soumyadeep Ghosh¹  Santosh S. Gupta¹ Nirad Mehta¹ Shanaz Khodajji²

¹Department of Imaging at Parmanand Deepchand Hinduja National Hospital and Medical Research Centre, Mumbai, Maharashtra, India

²Departments of Hematology and Transfusion Medicine at the Parmanand Deepchand Hinduja National Hospital and Medical Research Centre, Mumbai, Maharashtra, India

Address for correspondence Soumyadeep Ghosh, DNB, Department of Imaging at P. D. Hinduja National Hospital and Medical Research Centre, Mumbai, Maharashtra, India (e-mail: soumyadeep92@gmail.com).

Indian J Radiol Imaging 2021;31:725–728.

Abstract

Keywords

- ▶ avascular necrosis
- ▶ bone marrow necrosis
- ▶ chemical shift imaging
- ▶ computed tomography
- ▶ COVID-19
- ▶ disseminated intravascular coagulation
- ▶ opposed phase
- ▶ magnetic resonance imaging
- ▶ opposed phase
- ▶ positron emission tomography
- ▶ signal intensity index

We report, herein, a rare case of vertebral bone marrow necrosis in a patient at 1-month post–novel coronavirus disease 2019 (COVID-19) pneumonia complicated with disseminated intravascular coagulation (DIC). The commonly observed radiological features on the imaging modalities like computed tomography (CT), magnetic resonance imaging (MRI), and 18-F fluorodeoxyglucose positron emission tomography (FDG PET) have been discussed here followed by a brief discussion on the role of in-phase and opposed-phase imaging in differentiating the disease from malignant infiltrative pathologies. Histopathological findings on bone marrow smear that confirm the diagnosis have also been illustrated.

Introduction

The novel coronavirus disease 2019 (COVID-19 pneumonia) patients typically present with fever, shortness of breath, and cough. However, musculoskeletal complaints are seldom encountered as red flags. Here, we report the first presumptive case of COVID-19–associated vertebral

(and also pelvic and femoral) bone marrow necrosis, a rare disorder that has been associated with malignancies, sickle cell anemia, and other infections but is yet to be illustrated through the role of imaging in COVID-19-recovered patients.

It is imperative to begin with a few anatomical pearls pertinent to our case for a comprehensive understanding of

DOI <https://doi.org/10.1055/s-0041-1735919>.
ISSN 0971-3026.

© 2021. Indian Radiological Association. All rights reserved.
This is an open access article published by Thieme under the terms of the Creative Commons Attribution-NonDerivative-NonCommercial-License, permitting copying and reproduction so long as the original work is given appropriate credit. Contents may not be used for commercial purposes, or adapted, remixed, transformed or built upon. (<https://creativecommons.org/licenses/by-nc-nd/4.0/>)
Thieme Medical and Scientific Publishers Pvt. Ltd., A-12, 2nd Floor, Sector 2, Noida-201301 UP, India

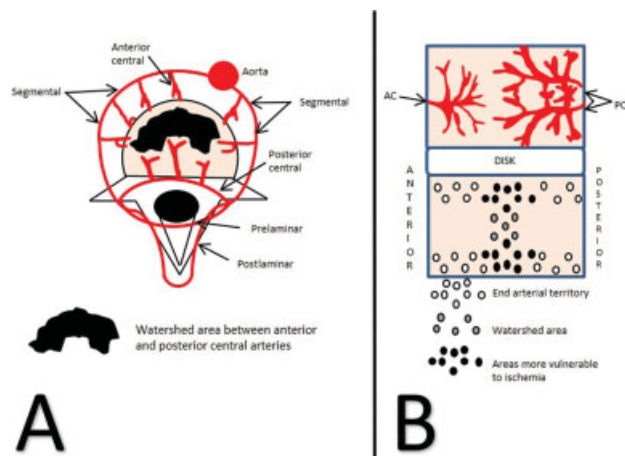


Fig. 1 (A) Axial schematic diagram of blood supply to bony vertebra showing anterior (AC) and posterior central (PC) arteries; black area represents watershed area between AC and PC arteries. (B) Midsagittal schematic diagram of two adjacent vertebral bodies with upper vertebra showing vascular territories of AC and PC arteries and lower vertebra showing watershed area (WSA; gray circles) in deep medullary portion and end arterial territory (EAT; white circles) near end plate. Black circles denote areas located within both EAT and WSA and may represent areas more vulnerable to ischemia.

the underlying radiological features (► **Fig. 1**). Each vertebral body is supplied mainly by anterior and posterior central arteries (central artery which supplies the vertebral centrum or body), whereas posterior element is supplied by pre- and postlaminar arteries. Posterior central arteries converge slightly posterior to the center of each vertebral body and supply central and posterior parts of each vertebral body. Anterior central arteries originate from segmental arteries directly and supply the anterolateral parts of each vertebral body. A watershed area exists in the deep medullary portion between the anterior and posterior central arteries.¹

Case Presentation

A 72-year-old male diabetic and hypertensive patient was admitted at an outside hospital, in mid-February of 2021, with the complaints of fever, cough, anosmia, and ageusia after his oral and nasopharyngeal swab reverse-transcription polymerase chain reaction (RT-PCR) assay was found to be positive. As per protocol, he received high-dose steroids, two doses of remdesivir which was discontinued on account of rising liver function tests. After spending 5 days there, he was shifted to our hospital where he received two doses of tocilizumab and was continued on high-dose intravenous dexamethasone. His blood sugar was controlled with human active insulin. His complete hemogram showed a decreasing platelet count which was tackled with platelet transfusions. Upon further investigation, it was detected that he had developed disseminated intravascular coagulopathy (DIC) due to *Klebsiella pneumoniae* sepsis for which filgrastim (for falling white blood cells [WBCs]) and meropenem (for *Klebsiella*) were initiated.

Ten days after his discharge from the COVID-19 unit, he presented with severe, radiating pain in both gluteal regions which aggravated both on sitting and walking. He was



Fig. 2 (A) STIR mid sagittal image showing hyperintensity in the anterior two-thirds and hypointensity in the posterior one-third of the vertebral bodies. (B) T1 mid sagittal image showing hypointensity in the posterior one-third of the vertebral bodies.

admitted in late March 2021 for this complaint and a whole spine screening magnetic resonance imaging (MRI) was performed which revealed abnormal marrow signal intensity in all vertebral bodies. Short-tau inversion imaging (STIR) and T1-hypointense areas with lack of signal drop on opposed-phase gradient images (signal intensity index [SII] of 1.0 or more; $SII = SI \text{ on opposed-phase image} / SI \text{ on in-phase image}$) were noted along the posterior third of all vertebral bodies. STIR hyperintensity was noted with an appropriate signal drop ($SII < 1.0$) on opposed-phase gradient images consistent with viable fatty marrow in the remaining anterior two thirds of the vertebrae (► **Figs. 2–5**).

Suh et al showed that in- and opposed-phase chemical shift imaging (CSI) has excellent diagnostic performance for differentiating benign and malignant vertebral bone marrow lesions with pooled sensitivity of 0.92 and specificity of 0.89. They found that the proposed signal intensity ratio cut-off values (opposed-phase–in-phase) were similar (0.8–1) in seven studies. They concluded that a signal intensity ratio of < 0.8 indicated significant signal drop on opposed-phase

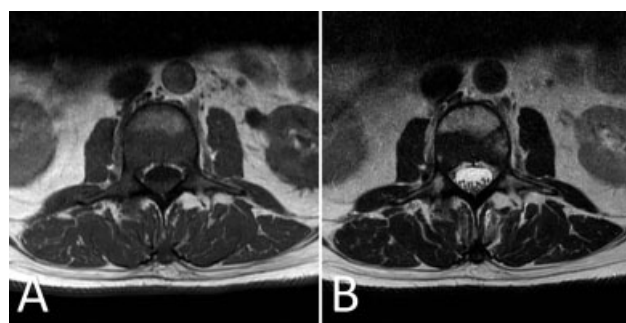


Fig. 3 Axial T1 (A) and T2 (B) images of L2 lumbar vertebra showing well-defined hypointensity on both T1 and T2 in the posterior one-third of the L2 vertebral body.

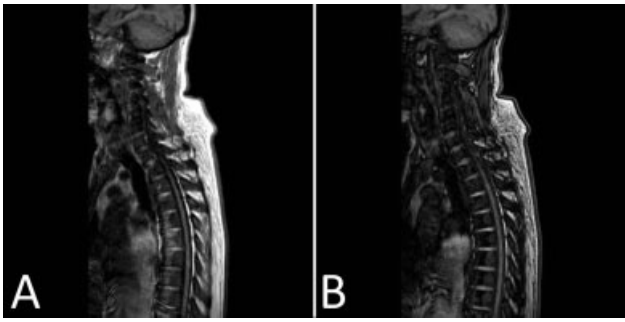


Fig. 4 In-phase (A) and opposed-phase (B) images of cervicodorsal spine showing signal drop on opposed-phase images in the anterior two-thirds of the vertebral bodies signifying viable fatty marrow.

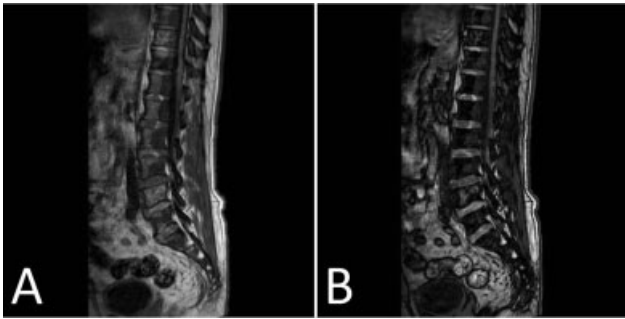


Fig. 5 In-phase (A) and opposed-phase (B) images of dorsolumbar spine showing signal drop on opposed-phase images in the anterior two-thirds of the vertebral bodies signifying viable fatty marrow.

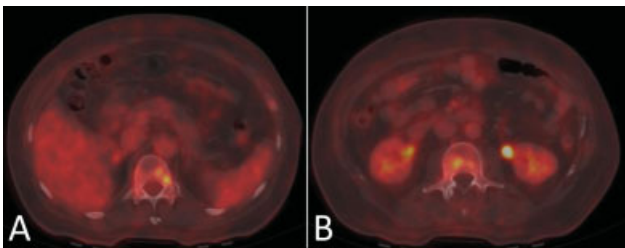


Fig. 6 18-F FDG PET-CT fusion images (A and B) showing heterogeneously increased tracer uptake in the posterior parts of vertebral bodies. CT, computed tomography; FDG PET, fluorodeoxyglucose positron emission tomography.

images and the presence of bone marrow fat, which favors a benign condition as fatty replacement, is associated with acute benign conditions. However, a signal intensity ratio >1 did not always mean that a malignancy is present but stem from increased amounts of blood and cell water.²

To further evaluate the condition, the patient underwent 18-F fluorodeoxyglucose positron emission tomography-computed tomography (FDG PET-CT) which demonstrated abnormal heterogeneous areas of increased tracer uptake in all the vertebral bodies (—Fig. 6) and showed mild sclerotic density with loss of normal trabecular pattern on CT corresponding to the abnormal T1 hypointense areas seen on the whole spine MRI (—Fig. 7). This was suggestive of an infiltrative marrow disorder or metastasis. The differential of avascular bone marrow necrosis was included to cover the imaging spectrum of morphological appearances. FDG uptake has been

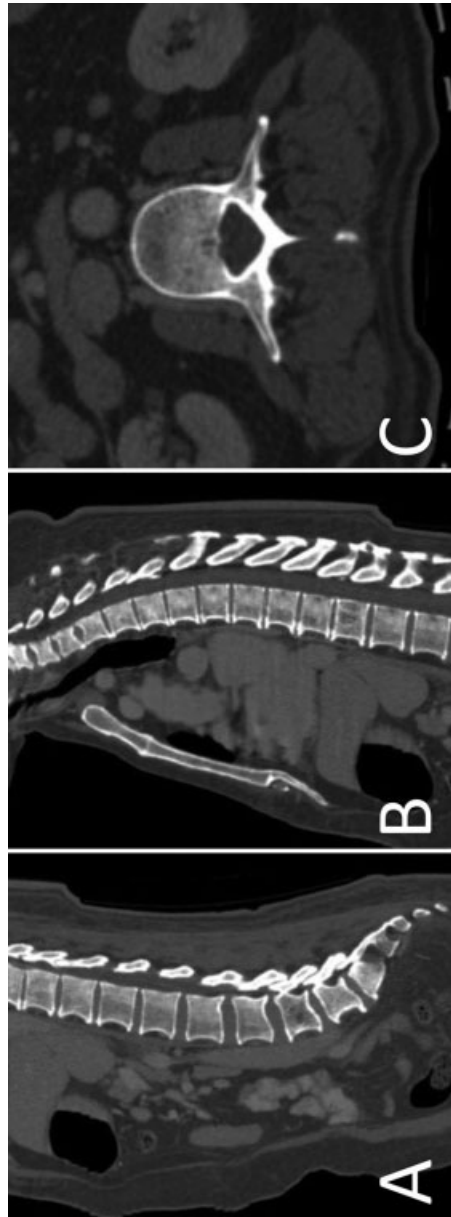


Fig. 7 Reformatted mid-sagittal (A, B) and axial (C) CT images showing mild sclerotic density with loss of normal trabecular pattern in the posterior parts of the vertebral bodies corresponding to the abnormal T1-hypointense areas seen in —Fig. 2. CT, computed tomography.

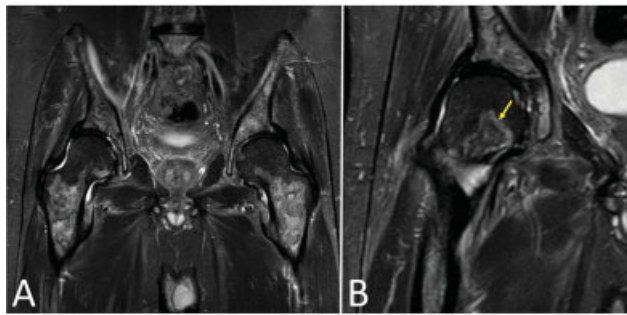


Fig. 8 (A, B) Coronal STIR screening sequence of pelvis with both hips showing well demarcated serpiginous STIR hyperintensity in both femora with the well-described “double line sign” (yellow arrow). STIR, short-tau inversion imaging.

reported in a case of avascular marrow necrosis by Grigolon and Delbeke. It is well reported that FDG tracer is taken up in inflammatory or infectious processes akin to the inflammatory exudates occurring in the pathogenesis of osteonecrosis.³ Sharply defined serpiginous areas of STIR hyperintensity were also noted in both halves of his pelvis and both femora, with presence of the well-described “double line sign,” suggestive of avascular bone necrosis (→Fig. 8).

This diagnostic conundrum, therefore, necessitated bone marrow trephine aspiration and biopsy which demonstrated areas of necrosis with neutrophilic debris, lymphohistiocytic aggregates, and proliferating fibroblasts in an oedematous background (→Fig. 9). Scattered reactive plasma cells showing immunopositivity for CD138 (cluster of differentiation), kappa and lambda immunostains were noted. An ill-formed granuloma comprising of lymphocytes, plasma cells, and few histiocytic cells was also seen.

COVID-19-associated bone marrow necrosis has commonly been reported with use of glucocorticoids in the conditions such as acute respiratory distress syndrome (ARDS). Glucocorticoids are widely used to hinder the progression of acute lung injury and ARDS in patients with severe acute respiratory syndrome (SARS) and COVID-19.⁴ A host of studies scrutinizing the use of steroids in viral respiratory diseases showed expected complications of avascular necrosis and diabetes, increased mortality, and secondary infections in influenza and reduced clearance of viral particles in SARS and Middle East respiratory syndrome (MERS) coronavirus outbreaks.⁵

Patients plagued with the severe form of COVID-19 disease often find themselves faced with such challenges as

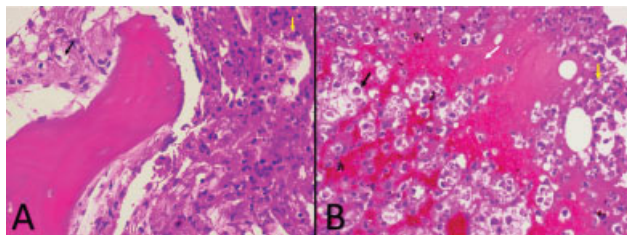


Fig. 9 (A, B) Bone marrow trephine biopsy sections (A and B; ×40 magnification) with hematoxylin & eosin stain show lymphohistiocytic aggregates (black arrow) and areas of necrosis (white arrow) with neutrophilic debris (yellow arrow) and proliferating fibroblasts in an oedematous background.

coagulopathies and DIC. Infection-induced endothelial dysfunction causes an excess of procoagulant thrombin with concomitant shutting down of the fibrinolytic cascade resulting in a hypercoagulable state which can spur thrombosis by increasing blood viscosity and coupled with hypoxia can activate the hypoxia-induced transcription factor-dependent signaling. To add to that, prolonged immobilization in these COVID-19 afflicted patients is associated with a much higher risk of developing venous thromboembolism.⁶

Conclusion

Based on the above clinical, radiological, PET, and bone marrow biopsy findings, we presume that the MRI features are highly suggestive of diffuse bone marrow necrosis associated with COVID-19 infection following treatment with high-dose pulse steroids. Our case report will help radiologists to consider bone marrow necrosis as a strong differential in the current pandemic as more of these kinds of rare observations of COVID-19 marrow involvement get reported.

Note

This article has not been presented or published anywhere else.

Funding

No support or funding has been requested or granted for this article.

Conflict of Interest

There is no conflict of interest.

Acknowledgment

I thank all the coauthors for the all the help and support rendered to make this report possible. I also take this opportunity to acknowledge the technologists and residents working in the departments of imaging in CT, MRI, and nuclear medicine subdivisions, as their work is an integral part of this article.

References

- 1 Yuh WT, Marsh EE III, Wang AK, et al. MR imaging of spinal cord and vertebral body infarction. *AJNR Am J Neuroradiol* 1992;13(01):145–154
- 2 Suh CH, Yun SJ, Jin W, Park SY, Ryu CW, Lee SH. Diagnostic performance of in-phase and opposed-phase chemical-shift imaging for differentiating benign and malignant vertebral marrow lesions: a meta-analysis. *AJR Am J Roentgenol* 2018;211(04):W188–W197
- 3 Grigolon MV, Delbeke D. F-18 FDG uptake in a bone infarct: a case report. *Clin Nucl Med* 2001;26(07):613–614
- 4 Horby P, Lim WS, Emberson JR, et al. RECOVERY Collaborative Group. Dexamethasone in hospitalized patients with Covid-19: preliminary report. *N Engl J Med* 2020;384(08):693–704
- 5 Marté JL, Toney NJ, Cordes L, Schlom J, Donahue RN, Gulley JL. Early changes in immune cell subsets with corticosteroids in patients with solid tumors: implications for COVID-19 management. *J Immunother Cancer* 2020;8(02):e001019
- 6 Dalro G, Silva ICF, Dalro PB, Silva ICF, Botelho VL. SARS-CoV-2/COVID-19 and its implications in the development of osteonecrosis. *J Regen Biol Med.* 2020;2(04):1–19